

STRUCTURAL CHANGES OF BAMBOO CELLULOSE IN FORMIC ACID

Yong Sun,¹ Lu Lin,^{1*} Haibo Deng,¹ Jiazhe Li,¹ Beihai He,¹ Runchang Sun,¹ and Pingkai Ouyang²

The structure of cellulose from bamboo fiber before and after treatment in formic acid was investigated in comparison with microcrystalline-cellulose by solid state NMR, FTIR, and X-ray diffraction diagrams. Differences of molecular structures among two kinds of celluloses were validated and expatiated. Results from the experiments indicated notable differences in the crystalline or amorphous region of microcrystalline-cellulose and bamboo fiber. CP-MAS ¹³C-NMR, and FTIR spectroscopy revealed the presence of I_α and I_β forms in all of the samples. The effect of acid solution was achieved simultaneously both in the crystalline region and the amorphous region, but there was a more intensive effect on the crystalline region for bamboo fiber. All of the cellulose samples revealed the same chain conformation but a different hydrogen bonding pattern. The absorbency of hydrogen bonds shifted to a high wave number and gradually decreased during treatment. The intermolecular hydrogen bond of 6-OH...O-3' decreased first, and then increased gradually, which indicated that the cellulose bundled together during hydrolysis.

Keywords: Microcrystalline-cellulose; Bamboo fiber; ¹³C CP/MAS; X-Ray; FTIR

Contact information: ¹State Key Laboratory of Pulp and Paper Engineering, South China University of Technology, Guangzhou, 510641, P.R. China; *Corresponding author: lclulin@scut.edu.cn (Lin)
²College of Medicine and Life Science, Nanjing University of Technology, Nanjing, 210009, P. R. China

INTRODUCTION

Cellulose, the most abundant renewable polymer available, is produced by nature at an annual rate of 10¹¹–10¹² tons (Hon 1994). If cellulose can be efficiently converted to monomeric sugars by hydrolytic processes, it can better compete with starch and play an important role to meet future energy needs. Regardless of one's purpose for doing hydrolysis, a more fundamental understanding of the structure of cellulose and hydrolysis process would lead to improved methods for preparing cellulose for conversion into fuels or materials.

Cellulose is a polymer consisting of unbranched β (1→4) D-glucopyranosyl units. The cellulose chains have a strong tendency to aggregate to highly ordered structural entities due to their chemical constitution and spatial conformation. Atalla and Vanderhart (1984) discovered that the ordered region of native cellulose is a mixture of two crystalline modifications (cellulose I_α and I_β) that vary in proportion, depending on the source of the cellulose. In bacterial and algal cellulose the I_α form dominates, while in higher plants it is I_β (Hayashi et al. 1997; Hardy 1996; Vanderhart et al. 1984). An

understanding of the crystalline region was greatly expanded by the work of Nishiyama et al., using X-ray neutron fiber diffraction, in which they were able to identify the hydrogen bonding network of I_{α} and I_{β} cellulose, the two naturally occurring crystal phases (Nishiyama et al. 2003, 2002). In addition to the crystalline regions (highly ordered), cellulose also contains amorphous regions. Thereby, a two-phase model with regions of high order and regions of low order was proposed (Earl et al. 1981). More recent models employ architectures of fibrillar units. Common structure schemes include skin and core networks, crystallinity of the surface and core has also been examined (Wickholm et al. 1998; Vanderhart et al. 1984).

The key to producing all kinds of chemical products is the depolymerization of cellulose to glucose, either chemically or enzymatically. The highly crystalline region is a main obstacle to break the β (1 \rightarrow 4) D-glucopyranosyl units. Thereby research has focused on the change of its molecular morphology during depolymerization (Coughlan et al. 1992), especially in understanding how morphology changes after differing amounts of hydrolysis have occurred. Since the early 1980s, high resolution solid-state NMR has become a powerful tool in the investigation of structural features of cellulose, especially of the crystalline ultrastructure. This technology is widely applied in understanding the change of cellulose by various treatments (Ibbett et al. 2007; Yunqiao et al. 2006; Sun et al. 2005; Hult et al. 2002; Zawadzki et al. 2002; Atalla et al. 1999; Hayashi et al. 1998; Guadalix et al. 1997; Yamamoto et al. 1993). Zawadzki and Yamamoto (Zawadzki et al. 2002; Yamamoto et al. 1993) employed cross polarization/magic angle spinning (CP/MAS) ^{13}C NMR technology to follow the evolution of chemical structure as a function of heat-treatment temperature. Pu and Hult (Pu et al. 2006; Hult et al. 2002) researched the change of supra-molecular structural features of cellulose by using CP/MAS ^{13}C NMR spectra in combination with line-fitting analysis. Different types of cellulose allomorphs (cellulose I_{α} , cellulose I_{β} , para-crystalline) and amorphous regions were hydrolyzed to different extents by the enzyme used. Infrared spectroscopy is a solid-state technique that can be used to identify cellulose samples of different origin and the change of hydrogen bonding; Sugiyama et al. demonstrated quite unambiguously that some infrared bands were specific for I_{α} , while others correspond to I_{β} cellulose (Sugiyama et al. 1991; Hayashi et al. 2005; Oh et al. 2005). Wide-angle X-ray diffraction usually gives the most direct information about the change of crystallinity. According to the two-phase structure theory, the crystallinity index (CI) is obtained from X-ray diffraction curves (Zhao et al. 2007; Oh et al. 2005).

Hydrolysis in formic acid solution is a novel pathway for conversion of lignocellulosic biomass into fermentable sugars (Sun et al. 2007). In this paper, X-ray diffraction (XRD), and CP/MAS ^{13}C solid-state NMR were used to follow the structural changes in microcrystalline-cellulose and bamboo fiber after various levels of hydrolysis. We directly observed and measured the crystallinity in cellulose (XRD, FTIR, and NMR). Examining the morphology before and after hydrolysis may help explicate the hydrolysis process, since the hydrolysis rate of the amorphous region is much higher than that of the crystalline region in cellulose (Zhao et al. 2006).

EXPERIMENTAL

Materials

The Microcrystalline-cellulose was purchased from the Shanghai Henxin Chemistry Company. Fiber materials were bleached sulfite bamboo pulps obtained from the Jiangmen Sugar Cane Chemical Factory (Group) Co., Ltd in China. Formic acid was purchased from the Shanhai Lingfeng Chemical Company and hydrochloric acid was purchased from the Guangdong Donghong chemical company in China.

Hydrolysis of Cellulose

In the experiment, 4g of fiber materials were placed in the reactor, which contained 96g formic acid solution (78.22 % (w/w) formic acid and 17.78 % (w/w) water), with additional hydrochloric acid at a ratio of 4% (w/w). The reaction was carried out at 65 °C. After reaction, formic acid and hydrochloric acid were extracted by a depressurization procedure. Then some water was put into the Erlenmeyer flask and filtered. The resulting solution was prepared for HPLC analysis. The remaining materials were adequately rinsed to neutral and subjected to freezing desiccation to ensure the complete removal of the formic acid.

HPLC Analysis

The HPLC system consisted of a Waters 600E system controller, Waters 717 automatic sampler, Waters 410 differential refractometer, and Waters Sugar pak I column. The mobile phase is pure water and was run at a flow rate of 1.1 ml/min. The LC system was operated at 90°C. The sample volume injection was 10 µL. Standard samples and hydrolyzate samples were filtrated by 0.45 µm filter and analyzed in duplicate.

X-Ray Diffraction Analysis

Wide-angle X-ray diffraction was conducted with a D/MAX-III, an instrument with 12° / min scan speed. Cellulose powder samples were laid on the glass sample holders (35×50×5 mm) and analyzed under plateau conditions. Cu radiation was generated at a voltage of 40 kV and a current of 30 mA. The scan scope was between 2° ~ 50°.

The degree of crystallinity (χ_c) was calculated by (Zhou et al. 2005; Focher et al. 2001):

$$\chi_c = F_c / (F_a + F_c) \times 100\% \quad (1)$$

where F_c and F_a are the area of crystal and noncrystalline regions, respectively.

The crystallite size was calculated from the Scherrer equation, with the method based on the width of the diffraction patterns. The crystallites sizes were determined from the 101, 002, and 021 lattice planes of cellulose samples,

$$D_{(hkl)} = \frac{K\lambda}{\beta_0 \cos \theta} \quad (2)$$

where $D_{(hkl)}$ is the size of crystallite (nm), K is the Scherrer constant (0.94), λ is X-ray wavelength, if copper target was used, and the λ is 0.15418 nm. β_0 is the full-width at half-maximum of the reflection hkl , measured in 2θ is the corresponding Bragg angle (Oh et al. 2005).

FTIR Analysis

FTIR spectra are recorded between 4000 and 400 cm^{-1} , using a NEXUS spectrometer with detector at 4 cm^{-1} resolution and 64 scans per sample. Discs have been prepared by first mixing 2 mg of dried sample with 200 mg of KBr (for spectroscopy) in an agate mortar. The resulting mixture was successively pressed at 10 MPa for 3 min.

^{13}C Solid State NMR

Cross polarization/magic angle spinning (CP/MAS) ^{13}C solid-state NMR experiments were performed on a Bruker Avance 400 spectrometer operating under the frequency of 100.61 MHz with 4 mm MAS BB-1H probe at 25 °C. The contact time for CP was 1.5 ms with a proton 90° pulse of 5.6 μs . The MAS speed was 5 kHz. The delay time after the acquisition of the FID signal was 3s.

The crystallinity (Cr.I.) and amorphicity (Am.I.) indexes, given as a percentage of the integrals of the C_4 peaks at 86–92 (a) and 80–86 ppm (b), were calculated by the following relations (Focher et al. 2001, Heux et al. 1999).

$$\begin{aligned} Cr.I.(%) &= 100 \times a / (a + b) \\ Am.I.(%) &= 100 - Cr.I. \end{aligned} \quad (3)$$

RESULTS AND DISCUSSION

CP-MAS ^{13}C -NMR Analysis

The CP/MAS ^{13}C solid-state NMR spectra of microcrystalline-cellulose and bamboo fiber are shown in Fig. 1. The resonance signals of the sample of being treated 3 hours were consistent to the control. Bamboo fiber treated for 3 hours displayed more distinct resonance peaks, and the overlapped peaks also became distinguishable. But for microcrystalline-cellulose, the peak didn't change. The main ^{13}C peak assignment values of two cellulosic materials are shown in Table 1. The peak assignments of C_1 , C_4 , and C_6 were confirmed by the technology of site-specifically labeling technique with ^{13}C and biosynthesis. But the $\text{C}_{2,3,5}$ peaks assignment did not reach an agreement (Witter et al. 2006, Kono et al. 2002, 2003, 2004).

Teeäär and Lippmaa (1984) had tried indirectly to assign the $\text{C}_{2,3,5}$ regions of the CP/MAS ^{13}C NMR spectrum of cotton cellulose (I_β -rich cellulose) based on a consideration of the ^{13}C spin-lattice relaxation times. They assigned the low-field doublet at 76.8 and 76.0 ppm to C_2 as the closest neighbor to the C_1 doublet. They also assigned the singlet line at 73.0 ppm to C_5 , and the remaining line at 74.2 ppm to C_3 , because the 74.2 ppm relaxed faster than the other lines in the cluster region. But Hiroyuki Kono and Shunji Yunoki (2002) thought the assignment of I_β subspectra, on the other hand, the doublet line at 76.8 and 76.0 ppm was directly assigned to C_3 by using the ^{13}C -labeled

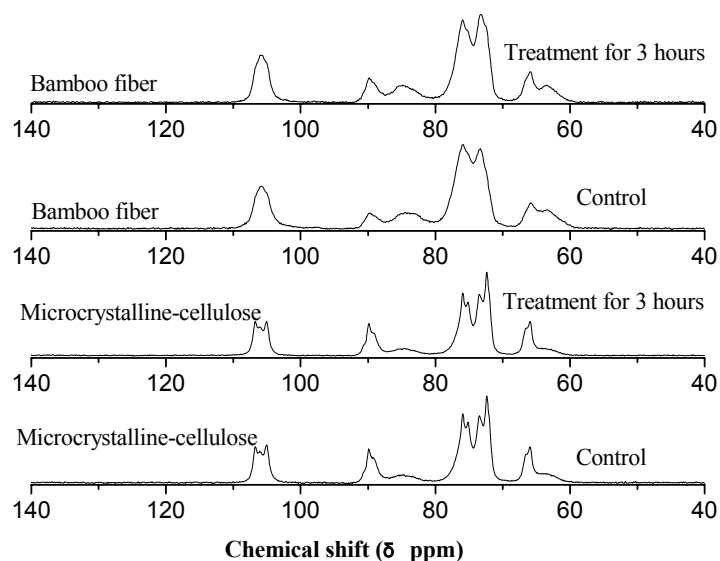


Fig. 1. CP/MAS ^{13}C NMR spectra of Microcrystalline-cellulose and Bamboo fiber.

cellulose biosynthesized from D-[1,3- ^{13}C] glycerol, which was also supported by the experiment of the ^{13}C labeled cellulose from D-[2- ^{13}C] glucose, and it was proved that the resonance lines for C_5 were split into a doublet in both subspectra of the I_α and I_β phases. For the assignment of the ^{13}C signal of cellulose in the solid state, Bardet et al (1997) applied the two-dimensional spin-exchange solid-state NMR technique to ^{13}C -enriched wood chips from aspen (*Populus euramericana*) grown under a 20% $^{13}\text{CO}_2$ atmosphere and observed the two broad signals around 76 and 74 ppm in the region of signals corresponding to C_2 , C_3 , and C_5 . They assigned the signal near 76 ppm to C_2 and that at 74 ppm to C_3 and C_5 by comparing the intensities of the signals as a function of increasing mixing time.

Table 1. Peak Assignment (ppm) values in ^{13}C -NMR Spectra of Bamboo Fiber and Microcrystalline-Cellulose

Samples	Control				Treatment for 3 hours			
	C_1	C_4	$\text{C}_{2,3,5}$	C_6	C_1	C_4	$\text{C}_{2,3,5}$	C_6
Bamboo fiber	105.853	84.375	75.917	65.844	106.005	89.825	75.948	65.917
		89.682	73.308	63.419		84.807	73.196	63.524
Micro-Crystalline cellulose	106.722	89.881	75.926		106.741		75.927	
	106.065	85.422	75.155		106.087	89.856	75.170	
	105.046	84.665	73.445	65.944	105.059		73.462	65.936
			72.362			84.773	72.370	

Although cellulose is a simple homopolysaccharide, it can exhibit a multitude of solid-state forms, depending on its origin and on the isolation methods used. The resonance line of microcrystalline-cellulose has some difference when compared with bamboo fiber. The main differences are around 105 ppm and 75 ppm. In the resonance line of microcrystalline-cellulose, there are three divided peaks at 105 ppm and four divided peaks at 75 ppm, but in the resonance lines of bamboo fiber, there only are the single peak at 105 ppm and two divided peaks at 75 ppm. The bamboo fiber is native cellulose, which is cellulose I consisting of cellulose I_{α} and I_{β} and so on (Horii et al. 1987). The NMR spectrum of bamboo fiber is consistent with much native cellulose, such as Soybean hulls, Endosperm, bleached Birch pulp, Flax, softwood Kraft, and so on (Focher et al. 2001; Heux et al. 1999; Wickholm et al. 1998). The NMR spectrum of microcrystalline-cellulose resembled that of ramie, cotton linters, hydrocellulose from cotton linters and so on (Atalla et al. 1999; Vander et al. 1984).

Though the solid-state structure differed widely between the samples, the most pronounced tendency through the series was the deterioration of spectral details from highly ordered to less-ordered cellulose. This was most clearly visible in the C_1 (δ 101-107ppm) and C_4 (δ 80-91ppm) regions of the spectra. The cellulose signal clusters were decomposed into contributing lines by a non-linear least-squares fitting of NMR spectra (Lorentzian fit), based on the quantification of the CP/MAS ^{13}C NMR spectra. The results of the non-linear least-squares fitting of the C_1 and C_4 regions of the microcrystalline-cellulose and bamboo fiber are shown in Figs. 2 and 3. The assignments and relative intensities are given in Table 2 and Table 3 (Larsson et al. 1995, 1997).

The most informative region in the NMR spectrum of cellulose is the signal cluster with a chemical shift distribution between δ 80 and 92 ppm. The fairly sharp signals from δ 86 to 92 ppm correspond to C_4 carbons from crystalline forms together with para-crystalline domains, whereas the broader upfield resonance line from δ 80 to 86 ppm is assigned to the amorphous domains (Larsson et al. 1997, 1999). Wickholm et al. (1998) and Larsson et al. (1999) think the region typical of the less ordered carbohydrate forms (80-86 ppm) contains several signals that are from the amorphous region and the accessible surface of cellulose; the signals of region (86-91 ppm) come from the crystalline region, the “in-core” fibre, and the inaccessible surfaces of cellulose.

Despite the apparent multiplicity of signals arising from the disordered regions, it was nevertheless possible to evaluate an “apparent crystallinity index” by integrating in the amorphous part of cellulose all contributions arising from the disordered regions, i.e. surface chains, crystal defects, and amorphous material, including hemicelluloses (Focher et al. 2001; Heux et al. 1999). From Table 3 one can see that the difference of all kinds morphology and the crystallinity index of microcrystalline-cellulose was 65.85%, higher than bamboo fiber. After treatment for three hours, the bamboo fiber increased 9.68%. But for microcrystalline-cellulose, the crystallinity index almost didn't change. Microcrystalline cellulose is a pure and highly crystalline cellulose; the consistency of crystallinity index before and after treatment by acid solution indicated that the hydrolysis simultaneously took place in the crystalline zone and amorphous zone. The bamboo fiber contained partly hemicellulose and lignin. During the hydrolysis, which could be dissolved and hydrolyzed, more surfaces were exposed. The effect of acid solution first was on the surface, and then simultaneously affected amorphous and

crystalline zones of fiber. The amorphous zone was more easily hydrolyzed than the crystalline zone, thereby the crystallinity index increased. Eventually the rigid framework of crystalline lattice of cellulose was crushed.

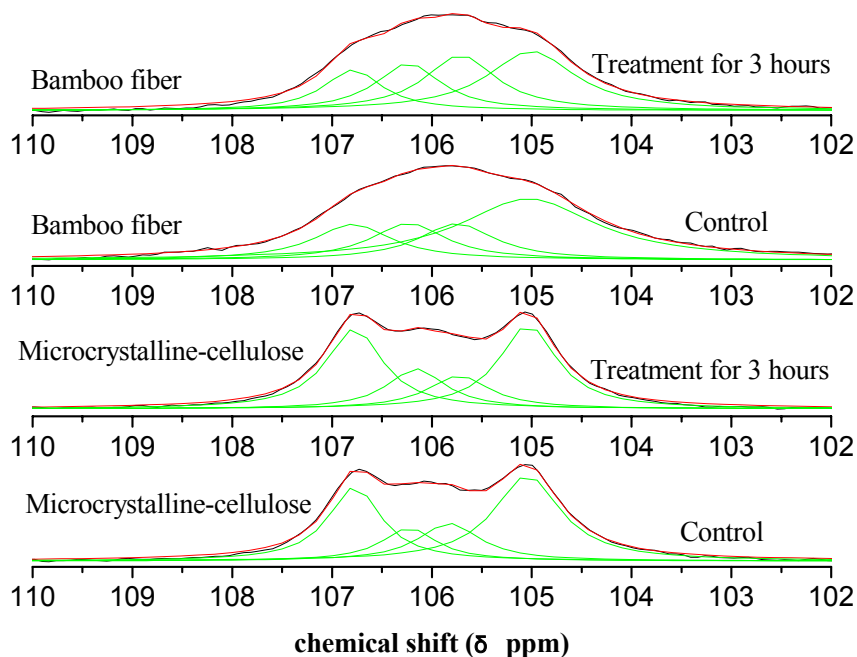


Fig. 2. Result of the fitting of the C₁ region of a CP/MAS ¹³C NMR spectrum from microcrystalline-cellulose and bamboo fiber. The chemical shift, relative intensity, and type of the individual lines are compiled in Table 1, respectively.

Table 2. Assignments and Intensity of a Non-linear Least-squares Fitting of the C-1 region of the CP/MAS ¹³C NMR Spectra

Material	Assignment	Control		Treatment for 3 hours	
		Chemical shift (ppm)	Intensity / %	Chemical shift (ppm)	Intensity / %
Micro-crystalline cellulose	I β	106.77	28.43	106.77	32.82
	I α	106.23	13.16	106.15	16.94
	Less-ordered	105.83	16.83	105.73	15.07
	I β	105.05	41.58	105.04	35.17
Bamboo fiber	I β	106.79	16.81	106.79	16.35
	I α	106.23	16.52	106.23	20.86
	Less-ordered	105.75	16.64	105.71	27.08
	I β	105.04	50.03	105.01	35.70

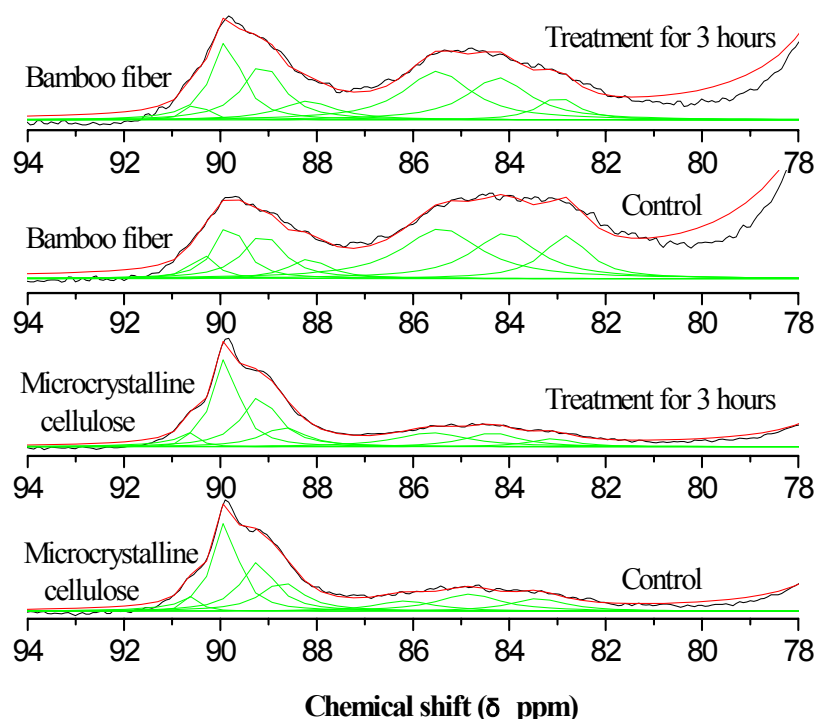


Fig. 3. Result of the fitting of the C₄ region of a CP/MAS ¹³C NMR spectrum from Microcrystalline-cellulose and bamboo fiber. The chemical shift, relative intensity and type of the individual lines are compiled in Table 1, respectively.

FTIR Analysis

Figure 4 shows the FTIR spectra of microcrystalline-cellulose and bamboo fiber. The most representative bands of microcrystalline-cellulose can be summarized as follows: The broad absorption at 3340–3412 cm⁻¹ related to the stretching of H-bonded OH groups, and one at 2968 cm⁻¹, 2900 cm⁻¹ to the C–H stretching (Wang et al. 2007; Pandey et al. 2005; Cao et al. 2004; Ivanova et al. 1989; Marchessault et al. 1962; Liang et al. 1959). The band at 1630 cm⁻¹ was attributed to the bending mode of the absorbed water (Cao et al. 2004). The bands at 1431 cm⁻¹ and 1316 cm⁻¹ in the spectrum were assigned to the symmetric CH₂ bending and wagging (Cao et al. 2004; Colom et al. 2003), the C–H bending occurs at 1373 cm⁻¹, 1281 cm⁻¹ (Colom et al. 2002). The absorption at 1201 cm⁻¹ belonged to the C–O–H in-plane bending at C-6, and the bands at 1237 cm⁻¹ was the bending of O–H (Oh et al. 2005; Fengel et al. 1991; Ivanova et al. 1989; Wiley et al. 1987; Marchessault et al. 1962). Two absorption bands at 1158 cm⁻¹ and 901 cm⁻¹ arose from C–O–C stretching at the β-(1→4)-glycosidic linkages (Cao et al. 2004; Hinterstoisser et al. 2001). The in-plane ring stretching gave a shoulder at 1114 cm⁻¹. Strong peaks at 1061 cm⁻¹ and 1033 cm⁻¹ were indicative of C–O stretching at C-3, C–C stretching and C–O stretching at C-6. A small peak at 672 cm⁻¹, 711 cm⁻¹ corresponded to

the out-of-plane bending of C-O-H (Liu et al. 2006; Oh et al. 2005; Fengel et al.1991; Wiley et al. 1987).

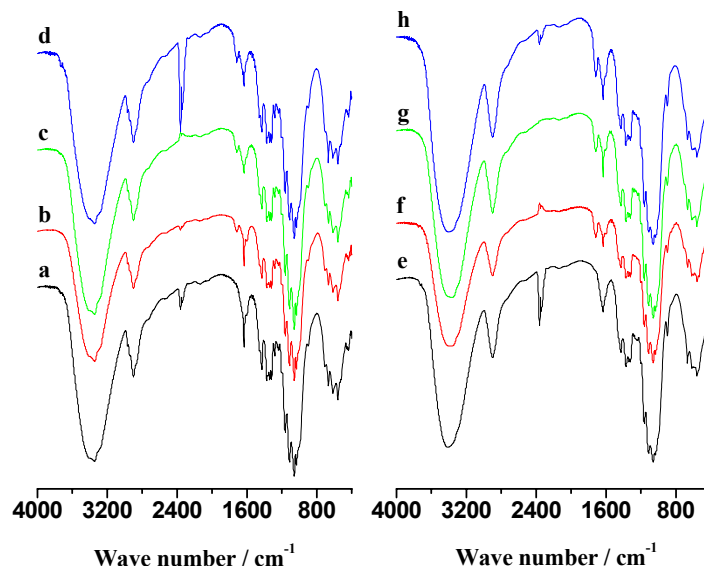


Fig. 4. FTIR spectra of microcrystalline-cellulose and bamboo fiber. a, b, c, d- the control and treatment for 1, 3, 5 hours of microcrystalline cellulose respectively. e, f, g, h- the control and treatment for 1, 3, 5 hours of bamboo fiber respectively.

The profiles of the FTIR spectra were very similar before and after treatment, whereas the intensity of peaks was different to some extent. For microcrystalline-cellulose, the absorbency at 901 cm^{-1} , 1033 cm^{-1} , 1114 cm^{-1} , 1158 cm^{-1} increased weakly, whereas at 1201 cm^{-1} , 1237 cm^{-1} , 1281 cm^{-1} , 1316 cm^{-1} , 1336 cm^{-1} , 1373 cm^{-1} , 1431 cm^{-1} , 2900 cm^{-1} it didn't change during treatment for 1 hour and 3 hours. This indicated that the effect of acid first was on the surface and amorphous zone, the hydrogen bonds were broken, and more bonds of types C-OH, C-O-C and C-C were exposed, thereby the stretching absorbency increased. After treatment for 5 hours, the absorbency at 901 cm^{-1} , 1033 cm^{-1} , 1114 cm^{-1} , and 1158 cm^{-1} weakly decreased, whereas at 1201 cm^{-1} , 1237 cm^{-1} , 1281 cm^{-1} , 1316 cm^{-1} , 1336 cm^{-1} , 1373 cm^{-1} , 1431 cm^{-1} it weakly increased. The number of stretching bonds C-OH, C-O-C and C-C decreased, and the bending and wagging of C-H, O-H and so on increased. This indicated the effect of acid solution eventually coming into the crystalline zone in the course of hydrolysis. For bamboo, the phenomena were like the microcrystalline-cellulose after treatment for 1 hour. After treatment for 3 hours, the phenomena were like the microcrystalline-cellulose after treatment for 5 hours. After treatment for 5 hours, all absorbency of peaks weakly decreased because of hydrolysis. The absorbency of $3400\text{--}3430\text{ cm}^{-1}$ decreased at all times, indicating the decrease of hydrogen bonds. At the same time, the absorbency around 3400 cm^{-1} weakly shifted to higher wave number, also indicating the rupture of hydrogen bonds (Cao et al. 2002). After treatment, the characteristic absorbency at 1718 cm^{-1} arose, showing that the formic acid had penetrated into the interior of cellulose and formed the new bond. There

was also some change at 1630 cm^{-1} because of the absorbance of water in atmosphere at different extent.

Table 3. Assignments and Intensity of a Non-Linear Least-Squares Fitting of the C-4 region of the CP/MAS ^{13}C NMR Spectra.

Material	Assignment	Control			Treatment for 3 hours		
		Chemical shift (ppm)	Intensity / %	Cr.I. / %	Chemical shift (ppm)	Intensity / %	Cr.I. / %
Microcrystalline cellulose	I α	90.59	2.92		90.60	2.92	
	I ($\alpha+\beta$)	89.89	29.29		89.89	31.52	
	Para-crystalline	89.22	21.42		89.18	24.81	
	I β	88.72	15.76	65.85	88.68	11.60	66.13
	Amorphous	86.17	7.79		85.61	14.01	
	Fibril surface	84.83	13.92		84.36	10.18	
	Fibril surface	83.40	8.90		83.12	4.96	
Bamboo fiber	I α	90.36	4.23		90.48	2.68	
	I ($\alpha+\beta$)	89.81	11.52		89.87	18.54	
	Para-crystalline	89.12	12.89		89.12	17.33	
	I β	88.17	5.74	30.54	88.19	8.22	40.22
	Amorphous	85.42	20.17		85.50	25.82	
	Fibril surface	84.09	26.17		84.23	20.62	
	Fibril surface	82.83	19.28		82.99	6.78	

In the spectra of microcrystalline-cellulose and bamboo fiber, there is an obvious absorption at 712 cm^{-1} and a weak absorption around 760 cm^{-1} . The bands around 760 cm^{-1} and 710 cm^{-1} were the characteristic absorption of cellulose I α and I β (Oh et al. 2005; Kataoka et al. 1999). This indicated that in two cellulose materials, both were rich in cellulose I β , and the microcrystalline-cellulose was more pure than the bamboo fiber. The NMR analyses also testify this point. After treatment, the absorbency decreased at all times, thereby increased for microcrystalline-cellulose after treatment for 5 hours.

Figure 5 shows the FTIR spectra of hydrogen-bonded O–H stretching vibrations with the correction of baseline. Assuming that all the vibration modes follow a Gaussian distribution, mixed modes of hydrogen bonded O–H stretching were resolved into three bands for all samples. Bands 1, 2, and 3 were related to the sum of the valence vibration of H-bonded OH groups and the intramolecular hydrogen bond of 2-OH \cdots O-6, the intramolecular hydrogen bond of 3-OH \cdots O-5, and the intermolecular hydrogen bond of 6-OH \cdots O-3', respectively (Oh et al. 2005) (Fig. 6).

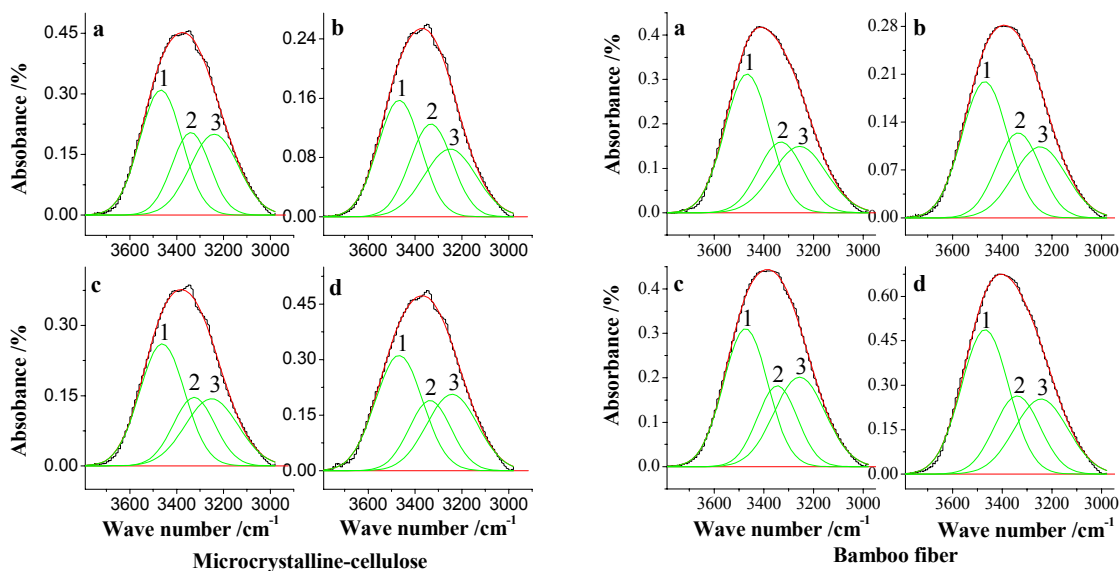


Fig. 5. Resolution of hydrogen-bonded OH stretching for microcrystalline-cellulose and bamboo fiber. a: control, b: treatment for 1 hours, c: treatment for 3 hours, d: treatment for 5 hours. 1: Valence vibration of H bonded OH groups and O(2) H-O(6) (intra), 2: O(3)H-O(5) (intra), 3: O(6)H-O(3') (inter).

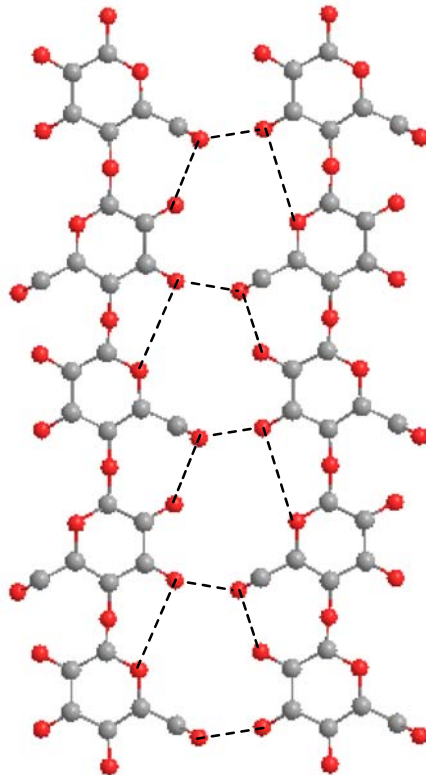


Fig. 6. Proposed hydrogen-bonding patterns of cellulose

Table 4 shows the values of the Cr.I. and lateral order indices (LOI) for two kinds of cellulose X-ray and NMR-analyses. The tests also revealed higher crystallinity values microcrystalline- cellulose than for bamboo fiber (Focher et al. 2001; Colom et al. 2003).

Table 4. Crystallinity Index (Cr.I.) and LOI of Microcrystalline Cellulose and Bamboo Fiber.

Samples	Treatment for	Cr.I. (%) (1373/2900 cm^{-1})	LOI (1430/895 cm^{-1})
Microcrystalline cellulose	Control	92.18	1.11
	1 hours	91.39	1.09
	3 hours	88.67	1.06
	5 hours	91.93	1.09
Bamboo fiber	Control	84.86	1.03
	1 hours	89.12	1.03
	3 hours	78.85	1.08
	5 hours	79.38	1.08

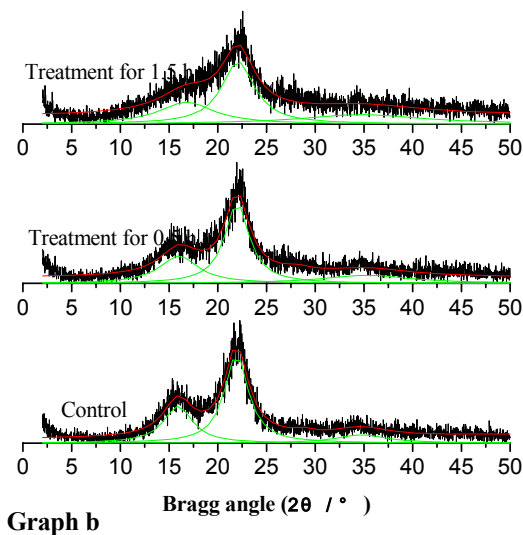
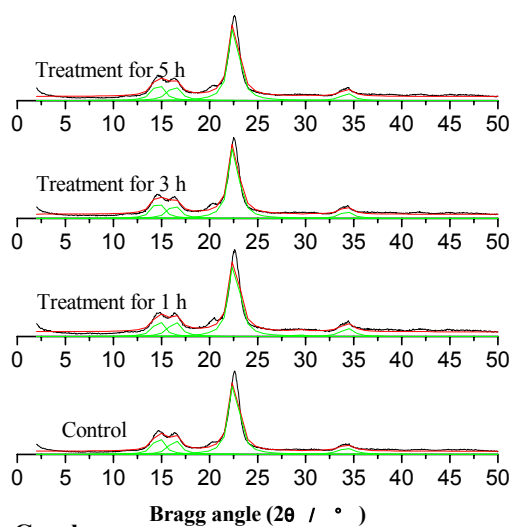
For microcrystalline-cellulose, the intensity of the intermolecular hydrogen bond of 6-OH...O-3' decreased after treatment for 1 hours, and then increased, which indicated firmer intermolecular hydrogen bonding and the breakdown of crystalline structure during hydrolysis (Table 5). The structure was loosened, the surface area increased, the surface energy also became large, the cellulose bundled together to decrease the surface free energy, and thereby the intermolecular hydrogen bond also increased. The phenomenon was the same for bamboo fiber.

X-Ray Diffraction Analysis

Figure 7 illustrates, for all the samples, the typical X-ray diffraction diagrams of the semi-crystalline cellulose allomorph. For microcrystalline-cellulose, the diffraction diagrams were well resolved and the degree of crystallinity and crystalline size could be seen to be higher than bamboo fiber (Table 6). The diffraction intensity of microcrystalline cellulose higher at all lattice planes than bamboo fiber. During the treatment, the cellulose gradually was hydrolyzed (Fig. 8), but the crystallinity degree of microcrystalline-cellulose didn't change. These observations indicated that the hydrolysis occurred simultaneously in the crystalline and amorphous zones. For the bamboo fiber, the crystallinity degree gradually decreased, which indicates that the effect of acid solution on crystalline zone was more than amorphous zone. The NMR analysis also testified to this point. The crystalline size of microcrystalline-cellulose didn't decrease, but for bamboo fiber, the change was large, especially for 101 crystalline lattice. The 101 and 002 lattice planes were regarded as the amorphous zone diffraction peak and crystalline zone, respectively, and the data corresponding to the crystalline size also attested to the effect of acid solution on the crystalline and amorphous zones simultaneously, though the effect of the crystalline zone was more than the amorphous zone.

Table 5. Assignments and Intensity of a Non-Linear Least-Squares Fitting of the Wave Number 3000~3800cm⁻¹ of the FTIR Spectra

Materials	Treatment for	Wave number /cm ⁻¹	Intensity /%	
Microcrystalline cellulose	Control	1	3467.3	42.90
		2	3339.3	25.46
		3	3238.9	31.63
	1 hours	1	3467.5	40.17
		2	3331.7	31.40
		3	3249.9	28.43
	3 hours	1	3461.7	46.27
		2	3325.4	23.94
		3	3250.6	29.79
	5 hours	1	3468.1	44.48
		2	3335.7	23.92
		3	3241.6	31.60
Bamboo fiber	Control	1	3467.9	47.90
		2	3332.7	24.74
		3	3255.4	27.37
	1 hours	1	3470.4	45.65
		2	3335.8	27.15
		3	3248.2	27.20
	3 hours	1	3473.7	43.92
		2	3346.1	23.23
		3	3256.4	32.85
	5 hours	1	3469.5	47.57
		2	3340.0	24.73
		3	3243.7	27.70

**Fig. 7.** The X-diffraction profiles of microcrystalline-cellulose and bamboo fiber. Graph a- microcrystalline- cellulose, Ggraph b- bamboo fiber

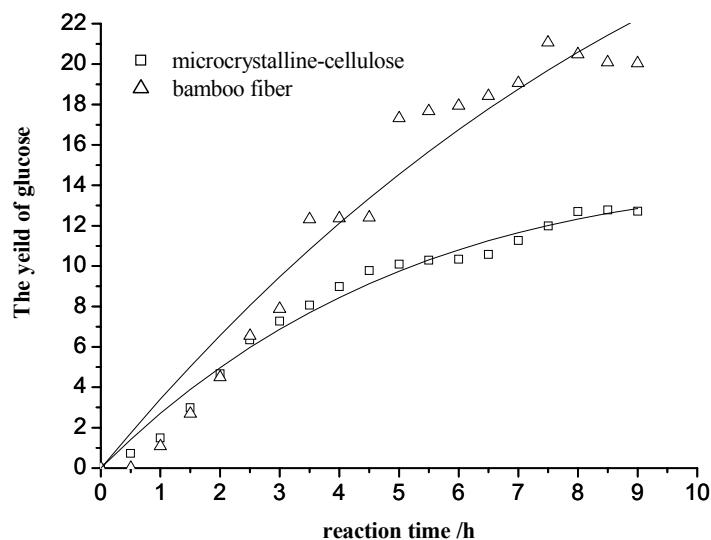


Fig. 8. Effect of reaction time (form 1h to 9h) on the release of glucose from microcrystalline cellulose and bamboo fibers in formic acid soln. (78.22 % formic acid and 17.78 % water) at 65°C

Table 6. The Characteristic X- Diffraction Peaks and Degree of Crystallinity of Microcrystalline Cellulose and Bamboo Fibers.

Material	Treatment for	lattice plane	Bragg angle $2\theta/^\circ$	Intensity / Cps	Crystalline size /nm	Crystallinity degree / %
Microcrystalline cellulose	Control	101	14.700	2706	6.74	62.48
		$10\bar{1}$	16.372	2471	6.47	
		020	22.587	9430	7.51	
		004	34.258	1209	4.68	
	1 hours	101	14.703	2181	6.83	63.13
		$10\bar{1}$	16.379	2157	5.94	
		020	22.596	7867	7.20	
		004	34.329	1440	5.62	
	3 hours	101	14.617	2479	6.55	62.28
		$10\bar{1}$	16.291	2249	6.22	
		020	22.529	8254	7.37	
		004	34.229	1239	6.05	
5 hours	101	14.657	2601	6.61	62.65	
	$10\bar{1}$	16.324	2299	5.70		
	020	22.568	8671	7.23		
	004	34.308	1359	5.98		
Bamboo fiber	Control	101	15.913	443	2.32	58.30
		020	21.930	862	2.88	
		004	34.766	205	1.34	
	0.5 hours	101	16.024	338	1.73	52.22
		020	21.985	742	2.79	
		004	35.264	177	0.78	
	1.5 hours	101	16.797	283	1.21	46.27
		020	22.091	646	2.06	
		004	34.879	196	0.57	

CONCLUSION

The NMR spectra of microcrystalline cellulose and bamboo fiber were found to be similar to most other native celluloses, and the proportion of cellulose I_{β} was larger than I_{α} . The crystallinity index (NMR) and degree of crystallinity of microcrystalline-cellulose was higher than bamboo fiber, indicating that the structure of bamboo fiber was looser than microcrystalline-cellulose. During the treatment, the yield of glucose gradually increased with the prolongation of reaction time, whereas the crystallinity index of microcrystalline-cellulose didn't change. In the case of bamboo fiber it gradually decreased. This indicated that the hydrolysis simultaneously took place in the crystalline zone and the amorphous zone. The X-ray diffraction data revealed this phenomenon. The FTIR spectra also attested to this point, since the stretching of hydrogen bonds of bamboo fiber arose at higher number than with microcrystalline-cellulose. These results also indicated that the structure of bamboo fiber was looser than microcrystalline cellulose. It follows that bamboo fiber should be easier to break down than microcrystalline-cellulose. The X-ray diffraction data also attested to this point. After treatment, the absorbency of hydrogen bonds stretching shifted to higher wave number and decreased to some extent, indicated the breaking of hydrogen bonds structure. The intermolecular hydrogen bond of 6-OH...O-3' decreased first, and then increased gradually, which indicated that the cellulose bundled together during hydrolysis. The reasons may be related to the removal of the non-cellulosic constituents, including hemicellulose and lignin, etc., and close packing of the chains. During the hydrolysis, the breakdown in structure and consequent crumbling also could result in the bundling of cellulose chains. The structure was loosened, the surface energy became large, and the new intermolecular hydrogen bond 6-OH...O-3' of cellulose formed to decrease the surface free energy. At the same time, the absorbency at 1000-1450 cm^{-1} also changed to different extents.

ACKNOWLEDGEMENT

The authors are grateful to the financial support from Natural Science Foundation of China (50776035, U0733001), Foundation of Scientific Research for Universities (20070561038) and Initiative Group Research Project(IRT0552) from Ministry of Education of China, National High Technology Project (863 project) (2007AA05Z408) and National Scientific Bracing Project (2007BAD34B01) from Ministry of Science and Technology of China.

REFERENCES CITED

- Atalla, R. H., and Vanderhart, D. L. (1984). "Native cellulose: A composite of two distinct crystalline forms," *Science* 223, 283–285.
- Atalla, R. H., and Vanderhart, D. L. (1999). "The role of solid state ^{13}C NMR spectroscopy in studies of the nature of native celluloses," *Solid State Nuclear Magnetic Resonance* 15(1), 1-19.

- Bardet, M., Emsley, L., and Vincendon, M. (1997). "Two-dimensional spin-exchange solid-state NMR studies of ^{13}C -enriched wood," *Solid State Nuclear Magnetic Resonance* 8(1), 25-32.
- Cao, Y., and Tan, H. (2004). "Structural characterization of cellulose with enzymatic treatment," *Journal of Molecular Structure* 705 (1-3), 189-193.
- Cao, Y., and Tan, H. (2002). "Effects of cellulose on the modification of cellulose," *Carbohydrate Research* 337(14), 1291-1296.
- Colom, X., and Carrillo, F. (2002). "Crystallinity changes in lyocell and viscose-type fibers by caustic treatment," *European Polymer Journal* 38(11), 2225-2230.
- Colom, X., Carrillo, F., Nogués, F., and Garriga, P. (2003). "Structural analysis of photodegraded wood by means of FTIR spectroscopy," *Polymer Degradation and Stability* 80(3), 543-549.
- Coughlan, M. P. (1992). "Enzymic hydrolysis of cellulose: An overview," *Bioresource Technology* 39(2), 107-115.
- Earl, W. L., and Vanderhart, D. L. (1981). "Observations by high-resolution carbon-13 nuclear magnetic resonance of cellulose I related to morphology and crystal structure," *Macromolecules* 14(3), 570-574.
- Fengel, D. (1993). "Influence of water on the hydroxyl valency range in deconvoluted FTIR spectra of cellulose," *Holzforschung* 47(2), 103-108.
- Fengel, D., and Ludwig, M. (1991). "Possibilities and limits of FTIR spectroscopy in characterization of cellulose. Part 1. Comparison of various cellulose fibers and bacterial cellulose," *Papier* 45(2), 45-51.
- Focher, B., Palma, M., Canetti, T., Torri, M., Cosentino, G. C., and Gastaldi, G. (2001). "Structural differences between non-wood plant celluloses: Evidence from solid state NMR, vibrational spectroscopy and X-ray diffractometry," *Industrial Crops and Products* 13(3), 193-208.
- Guadalix, M. E., Almendros, G., Martinez, A. T., Gonzalez-Vila, F. J., and Lankes, U. (1997). "A carbon- ^{13}C CP/MAS NMR evaluation of the structural changes in wheat straw subjected to different chemical and biological pulping conditions," *Bioresource Technology* 60(3), 245-249.
- Hardy, B. J., and Sarko, A. (1996). "Molecular dynamics simulations and diffraction-based analysis of the native cellulose fiber: Structural modeling of the I- α and I- β phases and their interconversion," *Polymer* 37(10), 1833-1839.
- Hayashi, N., Kondo, T., and Ishihara, M. (2005). "Enzymatically produced nano-ordered short elements containing cellulose I β crystalline domains," *Carbohydrate Polymers* 61(2), 191-197.
- Hayashi, N., Sugiyama, J., Okano, T., and Ishihara, M. (1998). "Selective degradation of the cellulose I α component in *Cladophora* cellulose with *Trichoderma viride* cellulose," *Carbohydrate Research* 305(1), 109-116.
- Hayashi, N., Sugiyama, J., Okano, T., and Ishihara, M. (1997). "The enzymatic susceptibility of cellulose microfibrils of the algal-bacterial type and the cotton-ramie type," *Carbohydrate Research* 305(2), 261-269.
- Heux, L., Dinand, E., and Vignon, M. R. (1999). "Structural aspects in ultrathin cellulose microfibrils followed by ^{13}C CP-MAS NMR," *Carbohydrate Polymers* 40(2), 115-124.

- Hinterstoisser, B., Åkerholm, M., and Salmén, L. (2001). "Effect of fiber orientation in dynamic FTIR study on native cellulose," *Carbohydrate Research* 334(1-3), 27-37.
- Hon, D. N.-S. (1994). "Cellulose: A random walk along its historical path," *Cellulose* 1(1), 1-25.
- Horii, F., Hirai, A., and Kitamaru, R. (1987). "CP/MAS carbon-13 NMR spectra of the crystalline components of native celluloses," *Macromolecules* 20(9), 2117-2120.
- Hult, E.-L., Liitia, T., Maunu, S. L., Hortling, B., and Iversen, T. (2002). "A CP/MAS ^{13}C -NMR study of cellulose structure on the surface of refined kraft pulp fibers," *Carbohydrate Polymer* 49(2), 231-234.
- Ibbett, R. N., Domvoglou, D., and Fasching, M. (2007). "Characterization of the supramolecular structure of chemically and physically modified regenerated cellulosic fibers by means of high-resolution Carbon-13 solid-state NMR," *Polymer* 48(5), 1287-1296.
- Ivanova, N. V., Korolenko, E. A., Korolik, E. V., and Zhbankov, R. G. (1989). "Mathematical processing of the IR spectrum of cellulose," *Zhurnal Prikladnoi Spektroskopii* 51(2), 301-306.
- Kataoka, Y., and Kondo, T. (1999). "Quantitative analysis for the cellulose Ia crystalline phase in developing wood cell walls," *International Journal of Biological Macromolecules* 24(1), 37-41.
- Kono, H., Erata, T., and Takai, M. (2003). "Complete assignment of the CP/MAS ^{13}C NMR spectrum of cellulose III_I," *Macromolecules* 36(10), 3589-3592.
- Kono, H., and Numata, Y. (2004). "Two-dimensional spin-exchange solid-state NMR study of the crystal structure of cellulose II," *Polymer* 45(13), 4541-4547.
- Kono, H., Yunoki, S., Shikano, T., Fujiwara, M., Erata, T., and Takai, M. (2002). "CP/MAS ^{13}C NMR study of cellulose and cellulose derivatives. 1. Complete assignment of the CP/MAS ^{13}C NMR spectrum of the native cellulose," *J. Am. Chem. Soc.* 124(25), 7506-7511.
- Larsson, P. T., Hult, E. L., Wickholm, K., Pettersson, E., and Iversen, T. (1999). "CP/MAS ^{13}C -NMR spectroscopy applied to structure and interaction studies on cellulose I," *Solid State Nuclear Magnetic Resonance* 15(1), 31-40.
- Larsson, P. T., Westermark, U., and Iversen, T. (1995). "Determination of the cellulose Ia allomorph content in a tunicate cellulose by CP/MAS ^{13}C -NMR spectroscopy," *Carbohydrate Research* 278(2), 339-343.
- Larsson, P. T., Wickholm, K., and Iversen, T. (1997). "A CP/MAS ^{13}C NMR investigation of molecular ordering in celluloses," *Carbohydrate Research* 302 (1-2), 19-25.
- Liang, C. Y., and Marchessault, R. H. (1959). "Infrared spectra of crystalline polysaccharides II: Native celluloses in the region from 640 to 1700 cm^{-1} ," *Journal of Polymer Science* 39, 269-278.
- Liu, C. F., Xu, F., Sun, J. X., Ren, J. L., Curling, S., Sun, R. C., Fowler, P., and Baird, M. S. (2006). "Physicochemical characterization of cellulose from perennial ryegrass leaves (*Lolium perenne*)," *Carbohydrate Research* 341(16), 2677-2687.
- Marchessault, R. H. (1962). "Application of infrared spectroscopy to cellulose and wood polysaccharides," *Pure and Applied Chemistry* 5, 107-29.

- Nishiyama, Y., Langan, P., and Chanzy, H. J. (2002). "Crystal structure and hydrogen-bonding system in cellulose I_β from synchrotron X-ray and neutron fiber diffraction," *Am. Chem. Soc.* 124(31), 9074-9082.
- Nishiyama, Y., Sugiyama, J., Chanzy, H., and Langan, P. (2003). "Crystal structure and hydrogen bonding system in cellulose I_α from synchrotron X-ray and neutron fiber diffraction," *J. Am. Chem. Soc.* 125(47), 14300-14306.
- Oh, S. Y., Yoo, D. I., Shin, Y., Kim, H. C., Kim, H. Y., Chung, Y. S., Park, W. H., and Youk, J. H. (2005). "Crystalline structure analysis of cellulose treated with sodium hydroxide and carbon dioxide by means of X-ray diffraction and FTIR spectroscopy," *Carbohydrate Research* 340(15), 2376-2391.
- Oh, S. Y., Yoo, D. I., Shin, Y., and Seo, G..(2005). "FTIR analysis of cellulose treated with sodium hydroxide and carbon dioxide," *Carbohydrate Research* 340(3), 417-428.
- Pandey, K. K. (2005). "Study of the effect of photo-irradiation on the surface chemistry of wood," *Polymer Degradation and Stability* 90(1), 9-20.
- Pu, Y., Cherie, Z., and Arthur, J. R. (2006). "CP / MAS ¹³C NMR analysis of cellulose treated bleached softwood kraft pulp," *Carbohydrate Research* 341(5), 591-597.
- Sugiyama, J., Persson, J., and Chanzy, H. (1991). "Combined infrared and electron diffraction study of the polymorphism of native celluloses," *Macromolecules* 24(9), 2461-2466.
- Sun, X. F., Xu, F., Sun, R. C., Fowler, P., and Baird, M. S. (2005). "Characteristics of degraded cellulose obtained from steam-exploded wheat straw," *Carbohydrate Research* 340(1), 97-106.
- Sun Y., Lin L., Pang C. S., Deng H. B., Peng H., Li J. Z., He B. H., and Liu S. J. (2007). "Hydrolysis of cotton fiber cellulose in formic acid," *Energy and Fuels* 21(4), 2386-2389.
- Teeäär, R., and Lippmaa, E.(1984). "Solid state carbon-13 NMR of cellulose. A relaxation study," *Polymer Bulletin* 12(4), 315-18.
- Vanderhart, D. L., and Atalla, R. H. (1984). "Studies of microstructure in native celluloses using solid-state carbon-13 NMR," *Macromolecules* 17(8), 1465-1472.
- Wang, L., Han, G., and Zhang, Y.(2007). "Comparative study of composition, structure and properties of *Apocynum venetum* fibers under different pretreatments," *Carbohydrate Polymers* 69(2), 391-397.
- Wickholm, K., Larsson, P. T., and Iversen, T.(1998). "Assignment of non-crystalline forms in cellulose I by CP/MAS ¹³C NMR spectroscopy," *Carbohydrate Research* 312(3), 123-129.
- Wiley, J. H., and Atalla R. H. (1987). "Band assignments in the Raman spectra of celluloses," *Carbohydrate Research* 160(15), 113-129.
- Witter, R., Sternberg, U., Hesse, S., Kondo, T., Koch, F.-T., and Ulrich, A. S. (2006). "¹³C chemical shift constrained crystal structure refinement of cellulose I_α and its verification by NMR anisotropy experiments," *Macromolecules* 39(18), 6125-6132.
- Yamamoto, H., and Horii, F. (1993). "CPMAS carbon-13 NMR analysis of the crystal transformation induced for *Valonia* cellulose by annealing at high temperatures," *Macromolecules* 26(6), 1313-17.

- Zawadzki, J., and Wisniewski, M. (2002). “ ^{13}C NMR study of cellulose thermal treatment,” *Journal of Analytical and Applied Pyrolysis* 62(1), 111-121.
- Zhou, D., Zhang, L., and Guo, S. (2005). “Mechanisms of lead biosorption on cellulose/chitin beads,” *Water Research* 39(16), 3755-3762.
- Zhao, H. K., Kwak, J. H., Wang, Y., Franz, J. A., White, J. M., and Holladay, J. E. (2006) “Effects of crystallinity on dilute acid hydrolysis of cellulose by cellulose ball-milling study,” *Energy & Fuels* 20(2), 807-811.
- Zhao, H. K., Kwak, J. H., Zhang, Z. C., Brown, H. M., Arey, B. W., and Holladay, J. E. (2007). “Studying cellulose fiber structure by SEM, XRD, NMR and acid hydrolysis,” *Carbohydrate Polymers* 6(2), 235-241.

Article submitted: December 7, 2007; Peer-reviewing completed: Jan. 16, 2008;
Revision received: Jan. 31, 2008; Revision accepted: Feb. 1, 2008; Published: Feb 10, 2008.